energies

MDPI

Article

Empirical Modeling of Synthetic Fuel Combustion in a Small Turbofan

Andrzej Kulczycki [1], Radoslaw Przysowa [1], Tomasz Białecki [1], Bartosz Gawron [1], Remigiusz Jasiński [2,*], Jerzy Merkisz [2] and Ireneusz Pielecha [2]

[1] Air Force Institute of Technology (ITWL), ul. Księcia Bolesława 6, 01-494 Warsaw, Poland; tomasz.bialecki@itwl.pl (T.B.); bartosz.gawron@itwl.pl (B.G.)
[2] Faculty of Civil and Transport Engineering, Poznan University of Technology, ul. Piotrowo 3, 60-965 Poznan, Poland; jerzy.merkisz@put.poznan.pl (J.M.); ireneusz.pielecha@put.poznan.pl (I.P.)
* Correspondence: remigiusz.jasinski@put.poznan.pl

Abstract: Drop-in fuels for aviation gas-turbine engines have been introduced recently to mitigate global warming. Despite their similarity to the fossil fuel Jet A-1, their combustion in traditional combustors should be thoroughly analyzed to maintain engine health and low emissions. The paper introduces criteria for assessing the impact of the chemical composition of fuels on combustion in the DEGN 380 turbofan. Based on previous emission-test results, the power functions of carbon monoxide and its emission index were adopted as the model of combustion. Based on the general notation of chemical reactions leading to the production of CO in combustion, the regression coefficients were given a physical meaning by linking them with the parameters of the kinetic equations, i.e., the reaction rate constant of CO and CO_2 formation expressed as exponential functions of combustor outlet temperature and the concentration of O_2 in the exhaust gas, as well as stoichiometric combustion reactions. The obtained empirical functions show that, in the entire range of engine operating parameters, synthetic components affect the values of the rate constants of CO and CO_2 formation. It can be explained by the change in activation energy determined for all chain-of-combustion reactions. The activation energy for the CO formation chain changes in the range between 8.5 kJ/mol for A0 and 24.7 kJ/mol for A30, while for the CO_2 formation chain between 29.8 kJ/mol for A0 and 30.8 kJ/mol for A30. The reactivity coefficient $\ln\alpha_{iCO}A_{CO}D_{CO}$ changes between 2.29 for A0 and 6.44 for A30, while $\ln\alpha_{iCO2}A_{CO2}D_{CO2}$ changes between 7.90 for A0 and 8.08 for A30.

Keywords: combustion modeling; exhaust emission; gas-turbine engine; chemical kinetic; sustainable aviation fuel; synthetic kerosene

Citation: Kulczycki, A.; Przysowa, R.; Białecki, T.; Gawron, B.; Jasiński, R.; Merkisz, J.; Pielecha, I. Empirical Modeling of Synthetic Fuel Combustion in a Small Turbofan. *Energies* **2024**, *17*, 2622. https://doi.org/10.3390/en17112622

Academic Editors: Haifeng Liu, Zongyu Yue and Chao Jin

Received: 21 April 2024
Revised: 25 May 2024
Accepted: 27 May 2024
Published: 29 May 2024

1. Introduction

Since the mid-20th century, jet fuels for gas-turbine engines, based on kerosene, have been produced with the two technologies of crude-oil processing: hydrorefining and Merox. Hydrorefining is based on a catalytic hydrogen process, in which sulfur is removed and double bonds are saturated between bonds. Merox technology is the catalytic oxidation of sulfur compounds. These two technologies, which differ significantly in the processes involved, make it possible to obtain fuels with a similar hydrocarbon composition and similar physicochemical properties. The following groups of hydrocarbons are basic components of jet fuels: paraffin~25%, isoparaffins~35%, cycloparaffin~20%, and flavors~20%. Conventional jet fuels have proven themselves in flight in terms of performance and safety. The need to reduce the emissions of greenhouse gases also from the aviation sector resulted in undertaking efforts to develop alternative fuels for aviation, most of which include components derived from biomass [1]. Biofuels produced using biomass are regarded as a renewable energy source and part of a closed carbon cycle in nature, so the CO_2 emitted during their combustion is not taken into account. Sustainable aviation fuels (SAF) are standardized biofuels for gas-turbine engines that have been introduced to mitigate global

warming [2–4]. They are assumed to be essentially identical to the standard jet fuel (Jet A-1) and referred to as drop-in fuels [5]. SAF fuels contain a dozen hydrocarbons belonging to paraffins and isoparaffins, while Jet A-1 fuel contains about a thousand hydrocarbons, including aromatics and naphthenes.

Differences in chemical composition between SAF and regular jet fuel cannot be completely ignored for safety reasons. Therefore, using these biofuels in civil aviation requires approval by both engine and aircraft manufacturers. The ASTM D4054 standard established the system for the certification of alternative jet fuels [6]. For each platform, a four-tier qualification process has to be followed for an individual alternative fuel [7]. In its wake, blends up to 50% SAF are approved by many original equipment manufacturers (OEMs) [8]. Recent efforts are focused on moving towards 100% SAF, but they are hampered by insufficient feedstock availability [9].

The development of aeroengines mainly involved their design and materials. Fuel was treated as a fixed element. Hence, in various engine models, the properties and chemical composition of the fuel are considered to a small extent. Nowadays, when biofuels and electrofuels [10–12] are introduced to aviation, the chemical composition and properties of the propellant cannot be assumed as fixed. Therefore, there was a need to develop new and improved tools for testing and modeling combustion when fuels of varied chemical composition are used [13–17].

Testing alternative jet fuels relies on a limited set of sensors for engine performance and emissions. Consequently, combustion is characterized by a small number of macroscopic parameters, which do not indicate subtle effects related to the chemical composition of fuels. In our prior tests [18,19], some minor deviations of engine operational parameters and emissions from the reference were found, but the reasons for the observed regularities were not well explained. To assess the impact of biofuels on engine operation, the mechanism and kinetics of the combustion reaction need to be considered. For combustion modeling in jet engines, several kinetic-based approaches are used, e.g., [20,21]. However, these models do not describe the cause-and-effect relationships between the kinetics of combustion and engine operation. Some teams conduct research in this direction [22], but the proposed models either require a description of individual reactions in fuel combustion chains or are based on statistical methods. In this case, empirically determined parameter values cannot be physically interpreted, and these values refer only to a limited group of fuels.

In chemistry, reactivity is understood as an impulse by which a substance reacts with a complete release of energy. We introduced a so-called α_i reactivity model, which combines the parameters related to the flow of energy with the quantities describing the kinetics of chemical reactions [23]. The general nature of the model, which considers both the flow of energy across the system boundaries (thermodynamic processes) and the kinetics of chemical reactions, makes it possible to describe combustion in gas-turbine engines. Attempts to apply the α_i reactivity model to analyze the combustion of fuel blends containing synthetic components were performed at the GTM 140 microturbine, which acted as an instrumented combustion rig. The reactivity model stands out by linking a thermodynamic process, such as engine operation, with a function that characterizes the kinetics of chemical reactions, enabling the process to occur.

This article applies the reactivity model in a turbofan engine to describe the combustion of fuel blends containing SAF in various concentrations and assesses the impact of fuel composition on turbine operation. The specific objective is to empirically determine the value of activation energy for the reaction chains of complete and partial combustion, as well as the values of reactivity coefficient α_i for blends of Jet A-1 fuel and the tested SAF.

2. Combustion Modeling

2.1. Chemical Kinetics in Combustion

Fuel combustion in gas-turbine engines is a chain of chemical reactions that vary greatly with the operating point of the engine. There are several modeling approaches based on physics and chemistry, e.g., [24]. While thermodynamics, fluid dynamics, and

other physical processes play a key role in achieving optimum combustion performance, chemical processes are important mainly for their impact on pollutant emissions and the limits of lean light off and lean blowout at high altitudes [25]. For a chemical reaction, its reaction rate v depends on the concentration of each reactant X and Y. The exponents p and q are reaction orders, which depend on the reaction mechanism:

$$v = k[X]^p[Y]^q \quad (1)$$

The reaction rate constant k is expressed by the Arrhenius equation as an exponential function of the temperature at which the reaction occurs. This is a fundamental formula for chemical kinetics based on the concept of activation energy E_a:

$$k = A \exp(-E_a/RT) \quad (2)$$

where: A is the Arrhenius pre-exponential factor, R is the universal gas constant, E_a is the activation energy for the reaction, and T is the absolute temperature.

The Arrhenius equation is often used in the linear form:

$$\ln k = -E_a/RT + \ln A \quad (3)$$

The Rice–Ramsperger–Kassel–Marcus (RRKM) model is based on the theory of chemical reactivity [26,27]. This method enables the computation of simple estimates of the unimolecular reaction rates from a few characteristics of the potential energy surface. The RRKM model describes the energy dependencies that determine the course of chemical reactions much better than the Arrhenius model. The microcanonical rate constant is expressed as:

$$k(E) = \sigma N^{++}(E - E_0)/h\ \rho(E) \quad (4)$$

where k(E) is the microcanonical rate constant and σ is the degeneracy of the reaction pathway. E is the internal energy of the system, E_0 is the activation energy for the reaction, $N^{++}(E - E_0)$ is the sum of states of the transition state from E_0 to E, ρ(E) is the density of states of precursors at energy E, and h is Planck's constant.

Other well-known models are dedicated to fuel combustion processes in internal combustion engines. For example, the SAE Aerospace Recommended Practice ARP 1533 [28] introduces a procedure for analyzing and evaluating the chemical composition of gaseous emissions from aircraft engines. Measurements of the CO_2, CO, NO_x, and C_xH_y emissions are used to determine:

- emission indices;
- fuel–air ratio;
- combustion efficiency;
- thermodynamic properties of exhaust gases.

The SAE procedure has been developed for turbine aircraft engines, but it can be applied to any other machines in which fuel combustion occurs. The basis of this model is the following chemical reaction:

$$\begin{aligned} C_nH_mOpN_qS_r + X[R(O_2) + S(N_2) + T(CO_2) + h(H_2O) + U(CH_4)] \rightarrow\ & P1(CO_2) + P2(N_2) \\ & + P3(O_2) + P4(H_2O) + P5(CO) + P6(C_xH_y) + P7(NO_2) + P8(NO) + P9(SO_2) \end{aligned} \quad (5)$$

The SAE procedure considers only a few selected properties of the fuels, which are mixtures of numerous individual chemical compounds. It is known, however, that combustion consists not only of the combustion reaction chains but of several sub-processes, e.g., the atomization of fuel. This process can be described by the Weber number defining the conditions for droplet atomization when aerodynamic forces and surface tension

equalize [27]. The atomization of the fuel stream into drops takes place when $We \geq We_{cr}$, where We is described by the equation:

$$We = \rho w^2 d / \sigma \quad (6)$$

where w is the initial droplet speed, ρ is the fluid density, d is the initial droplet diameter, and σ is the surface tension.

The critical value of Weber number We_{cr} is reached for critical droplet speed (maximum speed of a drop in a stationary gaseous medium, above which decay occurs) and depends mainly on liquid viscosity. The Weber number is a useful tool for estimating the droplet size in steady flows when the injection takes place into a medium in which there is no flow. In the case of unsteady flows, it was necessary to introduce corrective factors.

$$d = 6\sigma E_p - A_1 \eta v \quad (7)$$

where E_p is the fuel pulsation energy, A_1 is the constant volume, η is the dynamic viscosity, and v is the fuel flow velocity.

To a greater extent, the physicochemical properties of the fuel can be modeled in Ansys Chemkin-Pro software. For the simulation of reactions involving fuels, the model is supported by a fuel data library. Using this model, it is possible to calculate the thermodynamic effects of fuel combustion, i.e., the amount of heat released, the change in pressure in the combustion chamber, the flame propagation rate, and temperature in the combustion chamber. However, this model is based on relationships formulated using a large amount of experimentally obtained data. These data were used to determine the values of the relationship parameters using statistical methods. As a result, this model can be applied to a specific, relatively narrow group of fuels, and the introduction of new, yet unexplored, components may cause even large discrepancies between the model and the empirical data.

The models presented above are statistically formulated relationships combining, on the one hand, the physicochemical properties (e.g., density, distillation, and calorific value) of the fuel with the engine's operating parameters (e.g., thrust) and emissions of exhaust gas components. These models seem to bypass the combustion process and its chemistry. Cuoci et al. [29] reviewed models describing combustion in turbine engines. Among other things, the relationship between the mass flow rate and $\exp(E_a/RT)$ is presented, but the descriptions of the combustion process are either related to the chemical kinetics of the combustion reaction or describe the relationship between the engine operating (pressure, thrust, and temperature). A similar kinetic-based approach was proposed for propanol combustion by Wang et al. [30].

A number of advanced models have been developed to describe the kinetics of fuel combustion reactions, which take place in reactors of various designs. These models are formulated on the basis of tests of simple fuels in terms of chemical structure, such as hydrogen, methane, and single hydrocarbons. Curran et al. [20] reviewed models describing the combustion of hydrogen and individual hydrocarbons. They showed that some models describe chemical kinetics to a satisfactory extent and possibly combine them with elements of thermodynamics but do not allow for connecting combustion kinetics with engine operating parameters.

The concept that seems to be useful in combustion modeling is reactivity. In chemistry, it is understood as an impulse by which a substance reacts with a complete release of energy. Reactivity covers both thermodynamic factors and kinetic factors, which are actually different, and both usually depend on the temperature. Often, however, in chemistry, reactivity is equated with the rate of reaction.

2.2. Reactivity Model for Combustion

In this paper, the chemical reactivity of fuel blends containing synthetic components and the α_i model were used to describe combustion in an aviation turbine engine. The α_i reactivity model:

- links the function describing the flow of energy across the boundaries of the system with the function describing the change in the internal energy of the system resulting from chemical reactions taking place in the system;
- introduces a quantitative measure of reactivity in the form of the reactivity coefficient α_i.

The basic criterion for the model is the possibility of adopting one independent variable, e.g., fuel mass flow rate, on which the reactivity coefficient α_i will depend; all other quantities appearing in the model are functions of this variable. In general, the reactivity model can be presented as:

$$L = \alpha_i \, kD + L_0 \tag{8}$$

where L is generalized work done by the system (e.g., by engine proportional to thrust F) or on the system, L_0 is the constant value for the certain system and group of fuels, k is the constant rate of reaction taking place in the system, e.g., combustion reaction; and D is the change in the internal energy of the system caused by a chemical reaction undergoing with the rate appropriate to the unit value of the k.

A gas-turbine engine was adopted as the system studied in this work, and the dominant chemical reactions occurring in this system are related to fuel combustion. It can be assumed that the produced thrust F is linearly dependent on fuel flow:

$$F = a \, m_f + F_0 \tag{9}$$

where m_f is the fuel consumption, F_0 is the reference thrust value, constant for a given engine and fuel set, and a is the empirically determined proportionality coefficient.

If the α_i reactivity model describes the combustion of fuels blended in various concentrations, then the chain of chemical reactions taking place in the system can be expressed as:

- CO_2 and H_2O formation reaction:

$$C_xH_y + (x + y/4) \, O_2 \rightarrow x[CO_2] + y/2 \, H_2O \tag{10}$$

- CO and H_2O formation reaction:

$$C_xH_y + (x/2 + y/4) \, O_2 \rightarrow x[CO] + y/2 \, H_2O \tag{11}$$

- CO–to-CO_2 reaction:

$$CO + ½ \, O_2 \rightarrow CO_2 \tag{12}$$

The dominant reaction is the CO_2 formation, so Equation (8) can be presented as:

$$\alpha_{iCO2} = (L - L_0)/k_{CO2} \, D \tag{13}$$

where α_{iCO2} is the reactivity coefficient related to combustion to CO_2.

The work done by the system L is proportional to thrust F. So, assuming that L is related to the unit distance, the ($a \, m_f$) obtained from Equation (9) can be equal to ($L - L_0$).

$$L - L_0 = a \, m_f \tag{14}$$

Then

$$\alpha_{iCO2} = a \, m_f/k_{CO2} \, D \tag{15}$$

Based on Equation (1), the rate of fuel combustion to CO_2 and H_2O can be presented as:

$$d[CO_2]/dt = k_{CO2} \, m_f{}^p[O_2]^q \tag{16}$$

After integration in the limits <0, t>, the following relationship was obtained:

$$[CO_2] = k_{CO2} \, m_f{}^p[O_2]^q t \tag{17}$$

where p and q are effective reaction orders, t is the reaction time, m_f is the concentration of reaction substrates expressed as fuel flow, and O_2 is the oxygen concentration in the air flowing through the engine.

To estimate the reactivity coefficient α_{iCO2} for individual fuel blends, it was assumed that complete combustion takes place in the tested engine, so the entire amount of fuel is oxidized to CO_2.

By substituting k from the Arrhenius Formula (2) to Equations (15) and (17), the following was received:

$$\alpha_{iCO2ch}\, A_{CO2} \exp(-E_{aCO2ch}/RT) = (a/D_{CO2})m_f \tag{18}$$

$$[CO_2] = A_{CO2} \exp(-E_{aCO2ch}/RT_4)\, m_f{}^p [O_2]^q t \tag{19}$$

To model the dilution of combustion products by air flowing through the engine, the following functions are used:

$$\begin{array}{c} [CO_2]_{meas} = [CO_2]_{ch}/(AF) \\ \ln[CO_2]_{meas} = \ln[CO_2]_{ch} - \ln(AF) \end{array} \tag{20}$$

where AF is the air flow. Consequently, Equation (20) can be expressed as follows:

$$\ln[CO_2]_{meas} = -E_{aCO2ch}/RT_4 + p \ln(m_f[O_2]^q\, A_{CO2} t) - \ln(AF) =$$

$$-E_{aCO2meas}/RT_4 + p \ln(m_f[O_2]^q\, A_{CO2} t) \tag{21}$$

$$-E_{aCO2meas}/RT_4 = -E_{aCO2ch}/RT_4 - \ln(AF) \tag{22}$$

where $[CO_2]_{meas}$ is the CO_2 concentration measured in exhaust gases, E_{aCO2ch} is the activation energy resulting from the kinetics of the combustion reaction, without the effect of CO_2 dilution with air; $E_{aCO2meas}$ is the activation energy determined on the basis of $[CO_2]_{meas}$ measurements, and AF is the air low.

Equation (17) contains four measurable quantities. Three of them are dependent variables, namely thrust F, $[CO_2]$, and $[O_2]$, and one is an independent variable, namely fuel flow m_f. For a given fuel blend, the following dependencies can be empirically determined for engine operating points:

$$\begin{cases} F = f(m_f) \\ [CO_2] = g(m_f) \end{cases} \tag{23}$$

where $f(m_f)$ and $g(m_f)$ are the functions of fuel flow. By solving the system of equations, it will be possible to experimentally determine the value of α_{iCO2} for each tested fuel.

Respectively, for the fuel combustion reaction to CO, the following relationship can be formulated:

$$\alpha_{iCO} = (L - L_0)/k_{CO}\, D = a m_f/k_{CO}\, D \tag{24}$$

where α_{iCO} is the reactivity coefficient related to the fuel combustion reaction to CO. The rate of fuel combustion to CO and H_2O can be presented as:

$$d[CO]/dt = k_{CO}\, m_f{}^n [O_2]^r \tag{25}$$

After integration within the limits <0, t>, the following relationship was obtained:

$$[CO] = k_{CO}\, m_f{}^n [O_2]^r\, t \tag{26}$$

If CO can be treated as an intermediate product of the follow-up reactions in (10) and (11), the relationship between CO and mf can be expressed as:

$$[CO] = \{c_2 k_{CO}[1 + e^t]/e^t\, c_5 k_{CO2}\}\, m_f{}^n \tag{27}$$

After substituting Equation (13) into (9), the following was obtained:

$$\alpha_{iCO} = (L - L_0)/D([CO]m_f{}^{-n}[O_2]^{-r}\ t^{-1}) \quad (28)$$

As described by Åkerblom et al. [12], the kinetic of the CO creation during the combustion process can be described by the following kinetic equations:

(a) for parallel reactions:

$$[CO] = c_2 k_{CO}\ t\ m_f{}^{-n+1} \quad (29)$$

(b) for follow-up reactions:

$$[CO] = \{c_2 k_{CO}\ [1 + e^t]/e^t\ c_5 k_{CO2}\ \} m_f{}^n \quad (30)$$

where c_2 is the coefficient determining the participation of $[O_2]^{np(x/2+y/2)}$ in the rate of reaction (10) and c_5 is the coefficient determining the participation of $[O_2]^{np(x/2+y/2)}$ in the rate of reaction (11).

When CO is an intermediate product of fuel oxidation to CO_2, Equation (30) can be expressed as:

$$\ln[CO] = \ln c_{CO} - E_{aCO}/RT_4 + E_{aCO2}/RT_4 + n\ln m_f \quad (31)$$

where $c_{CO} = c_2[1 + e^t]/e^t c_5$.

The description of the kinetic of CO formation should consider the dilution of combustion products by air:

$$\begin{gathered} [CO]_{meas} = [CO]_{ch}/(AF) \\ \ln[CO]_{meas} = \ln[CO]_{ch} - \ln(AF) \\ [CO]_{meas} = \{c_2 k_{CO}\ [1 + e^t]/e^t\ c_5 k_{CO2}\} m_f{}^n/(AF) \\ [CO]_{ch} = (AF)\ [CO]_{meas} = (k_{CO}/k_{CO2})_{ch}\ \{c_2[1 + e^t]/e^t\ c_5\} m_f{}^n \end{gathered} \quad (32)$$

$$\ln[CO]_{meas} = (-E_{aCOch} + E_{aCO2ch})/RT_4 + \ln\{c_2[1 + e^t]/e^t\ c_5\} + \ln m_f{}^n - \ln(AF) \quad (33)$$

The values of E_{aCOch}/RT_{41} and am_f can be used for the $\alpha_{iCO}A_{CO}D_{CO}$ calculation.

$$\begin{gathered} \alpha_{iCO} = am_f/k_{CO}\ D_{CO} \\ \alpha_{iCO} = am_f/D_{CO}\ A_{CO}\ \exp[(-E_{aCO}/R)(1/T)] \\ \ln\alpha_{iCO} = \ln(am_f) - \ln(D_{CO}\ A_{CO}) + E_{aCO}/RT \\ E_{aCO}/RT = \ln\alpha_{iCO}\ D_{CO}\ A_{CO} - \ln(am_f) \end{gathered} \quad (34)$$

For a given fuel blend, the following dependencies can be empirically determined for the engine operating points:

$$\begin{cases} F = f(m_f) \\ [CO] = h(m_f) \end{cases} \quad (35)$$

where $f(m_f)$ and $h(m_f)$ are the functions of fuel flow. By solving the system of equations, it will be possible to experimentally determine the value of α_{iCO} for each tested fuel.

The proposed αi reactivity model describes the impact of the fuel chemical composition on the engine operation. Equations (2), (9), (13), and (24) will be used to characterize combustion and determine to what extent it is affected by adding biofuels to Jet A-1. Figures 1 and 2 summarize the methodology of E_{aCO2}, E_{aCO}, αi_{CO2}, and αi_{CO} determination as quantities characterizing fuel behavior during the combustion process. The parameters shown in Figures 1 and 2 were used to model the impact of component A on combustion in the DGEN 380 engine.

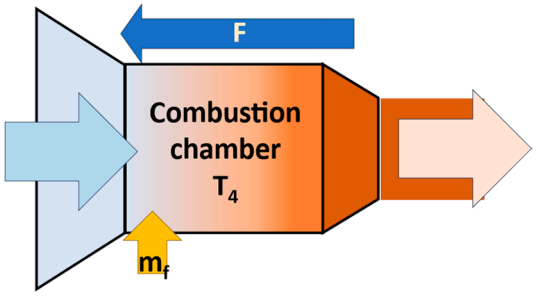

Figure 1. Variables used to estimate E_{aCO2ch} and αi_{CO2ch}.

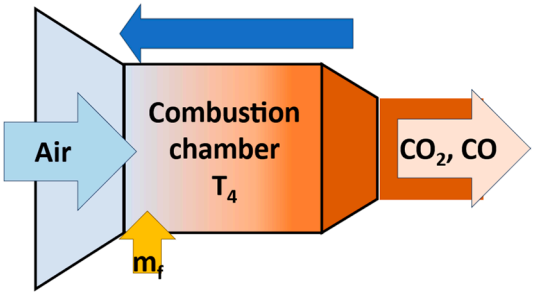

Figure 2. Variables used to estimate $E_{aCO2meas}$, $E_{aCOch,}$ and αi_{COch}.

3. Materials and Methods

3.1. Fuels

Blends of the commercial Jet A-1 fuel with synthetic components approved by ASTM D7566 (Table 1) were prepared. They were tested in the laboratory for their compliance with ASTM D7566 (Table 2).

Table 1. Volumetric composition of tested fuel blends.

Blend	Jet A-1	SAF
A0	100%	0%
A5	95%	5%
A20	80%	20%
A30	70%	30%
A	0%	100%

Table 2. Fuel lab-testing results.

Property	Unit	Requirement	Lab-Test Result				
			A0	A5	A20	A30	A
Density at 15 °C	kg/m^3	775–840	798	796	790	786	759
Viscosity at −20 °C	mm^2/s	max 8.0	3.40	3.45	3.57	3.66	4.78
Net heat of combustion	MJ/kg	min 42.8	43.2	43.3	43.4	43.4	44.0
Aromatics	(*v*/*v*)%	max 25	16.7	15.7	13.0	11.3	0
Naphthalenes	(*v*/*v*)%	max 3	0.58	0.55	0.46	0.40	
Flash point	°C	min 38	49.5	49.0	49.0	49.0	47.5
Freezing point	°C	max −40	−63.5	−65.5	−66.5	−66.8	−67.5
Smoke point	mm	min 18	20	23	25	28	

3.2. Engine Testing

The reactivity model was used to study the fuel combustion at the WESTT test cell with a Price Induction DGEN 380 engine. It is a small and high bypass ratio (7.6) geared turbofan (Figure 3), producing 255 daN (Table 3) of thrust while maintaining emissions and fuel consumption at a low level. It was developed by the French company Price Induction for educational and general aviation applications using modern, high-performance materials to ensure optimal performance and life. The turbofan design follows the more electric engine concept since it uses electrically driven oil and fuel pumps and an electrical starter–generator. The data-acquisition system of the WESTT test cell [31] enables data acquisition and the analysis of several engine performance parameters, such as thrust, fuel consumption, temperature, and pressure.

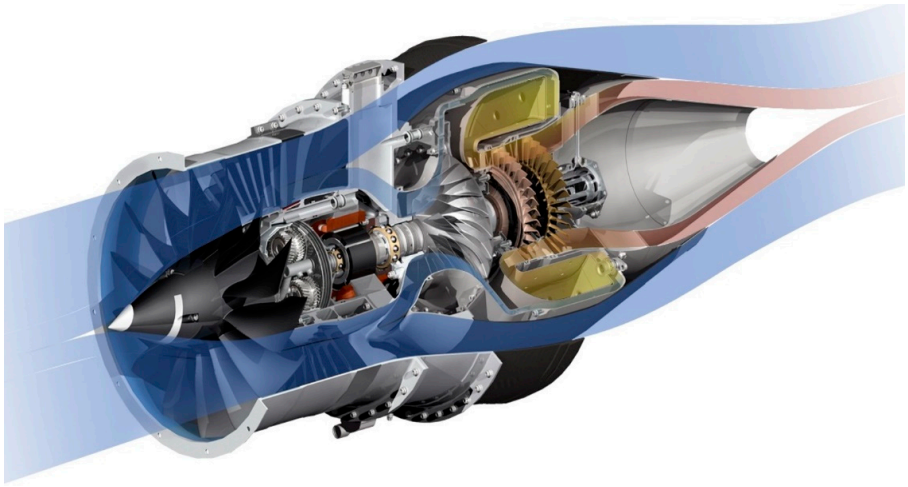

Figure 3. Price Induction DGEN 380 turbofan [32].

Table 3. Technical specification of the DGEN 380 turbofan [32].

Maximum Thrust	**255 daN**
Specific Fuel Consumption (for maximum thrust)	12.4 g/kN·s
Bypass ratio	7.6
Weight	85 kg
Lifetime	3600 h

In the engine test, a finite amount of fuel in the tank was used to maintain a constant blend ratio throughout the test. The engine dwelled at the selected operating points for a minute at least. Exhaust gases were measured with the Semtech DS analyzer through a probe maintaining the temperature of 191 °C. The concentration measurement of CO and CO_2 was performed with a non-dispersive infrared (NDIR) analyzer. The test procedure and emission measurements are presented in detail in [23]. The engine test profile is presented in Table 4.

Table 4. Test profile of DGEN 380 engine.

Step	Thrust [%]	Thrust [daN]	NH [%]	NL [%]	PLA [%]	Fuel Flow [L/h]	Operating Mode
1	10	26.4	52.7	33.5	0	32	Idle
2	13	33.8	57.8	37.8	11	37	
3	20	50.9	66.2	45.8	29	44	Cruise
4	26	65.8	74.9	57.3	57	49	
5	40	100.9	81.1	65.3	61	66	Max
6	56	141.6	87.7	75.3	75	86	
7	72	183.5	93.3	86.1	87	112	
8	97	246.3	99.3	99.4	100	151	Take-off

4. Results

4.1. E_{aCO2} and α_{iCO2} Determined from Engine Operating Parameters

The calculated activation energy and reactivity coefficients are based on the operational parameters of the engine, such as thrust, fuel flow, mass air flow, combustor outlet temperature and the emissions of CO, and CO_2. Figure 4 shows the linear dependency of mass flow m_f on thrust F (Equation (9)), while Table 5 presents the regression results. The obtained slope and intercept indicate that the A0 fuel (Jet A-1) has a slightly different thrust vs. the m_f function than its blends with component A. This may be due to the difference in the calorific value of the tested fuels, as well as a different hydrocarbon structure, which is visible already at 5% wt of component A.

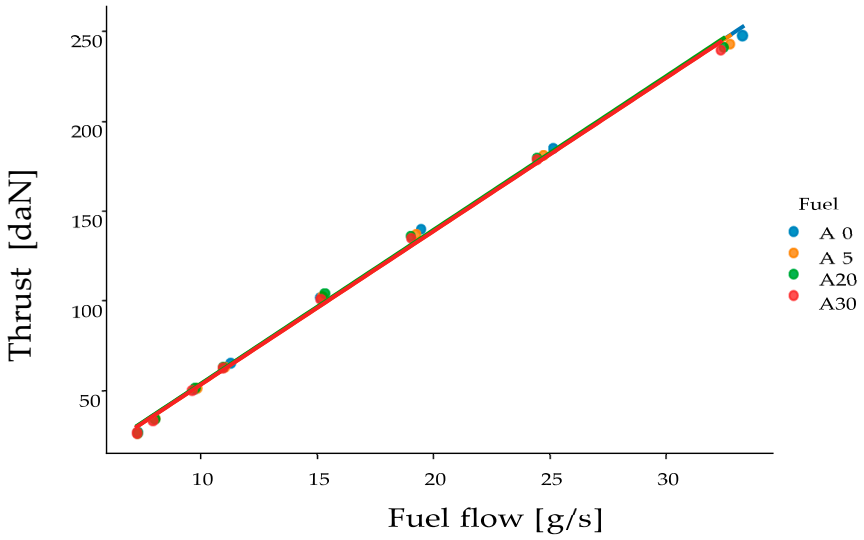

Figure 4. Thrust F as a function of fuel flow m_f for the tested blends.

Table 5. Regression results for thrust vs. mass flow.

Fuel	a	F_0	R^2
A0	6.123	18.7	0.9978
A5	6.384	25.11	0.9980
A20	6.397	24.7	0.9976
A30	6.374	24.98	0.9982

4.2. E_{aCO2ch} and αi_{CO2ch} Determined from Emission Measurements

For the tested blends, fuel flow was related to the inverted combustion temperature (Figure 5). The regression results are presented in Table 6.

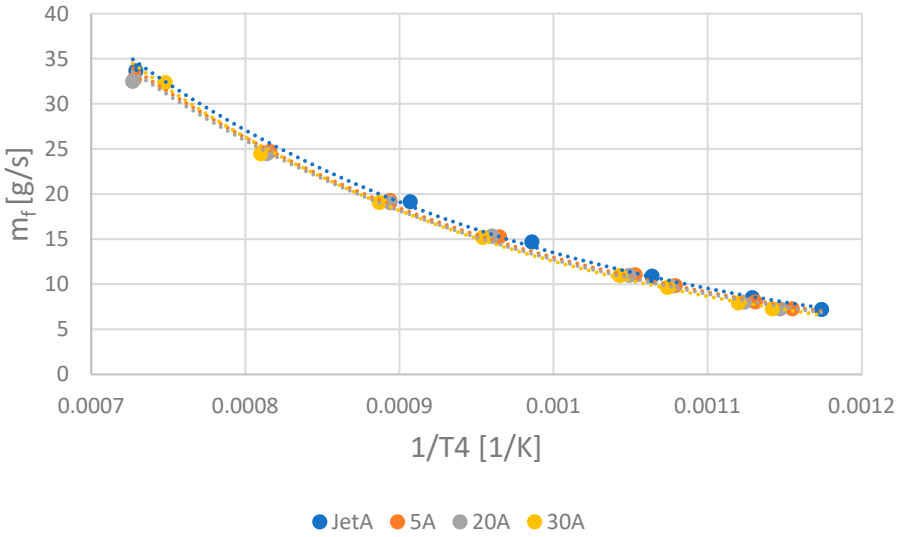

Figure 5. Fuel flow vs. inverted temperature.

Table 6. Regression results for fuel flow vs. inverted temperature.

Fuel	R^2	E_{aCO2ch}/R	E_{aCO2ch} [kJ/mol]	$(\alpha_{iCO2ch}A_{CO2}D/a)$	$(\alpha_{iCO2ch}A_{CO2}D_{CO2})$	$\ln(\alpha_{iCO2ch}A_{CO2}D_{CO2})$
A0	0.9979	3480	29.8	438.38	2684	7.90
A5	0.9977	3525	29.3	440.32	2811	7.94
A20	0.9973	3556	29.5	445.71	2851	7.96
A30	0.9978	3705	30.8	509.79	3249	8.08

The values of A_{CO2} and D_{CO2} should be constant for all tested fuels. A_{CO2} is a pre-exponential factor in the Arrhenius equation. Its value should be constant for a given reaction. In this research, it was assumed that the A_{CO2} value is constant for the chains of reactions undergone during the combustion process. D_{CO2} is the proportional coefficient describing the change in the internal energy of the system caused by a chemical reaction undergone at the rate appropriate to the unit value of the k. It was assumed the constant value of this coefficient for the tested fuels. Consequently, the differences in $(\alpha_{iCO2}A_{CO2}D_{CO2})$ result from different values of α_{iCO2}. The obtained results confirm that the reactivity coefficient α_i does not depend on the fuel mass flow rate and is a characteristic quantity for fuel with a specific chemical composition.

The values of the constant reaction rate of the combustion reaction of the tested fuels to CO_2 were also estimated from Equation (18). However, introducing the empirically determined concentrations of CO_2 and O_2 in the exhaust gases and m_f. The values of $a_{CO2;T} = A_{CO2}\ m_f O_2{}^p t$, and $E_{aCO2meas}/R$ were empirically determined. The results are presented in Figure 6 and Table 7. The curve for the A0 fuel has a different trend than the ones for blends containing component A. The values of EaCO2meas, quite different than those shown in Table 6, are the result of the dilution of combustion products by air flowing through the engine.

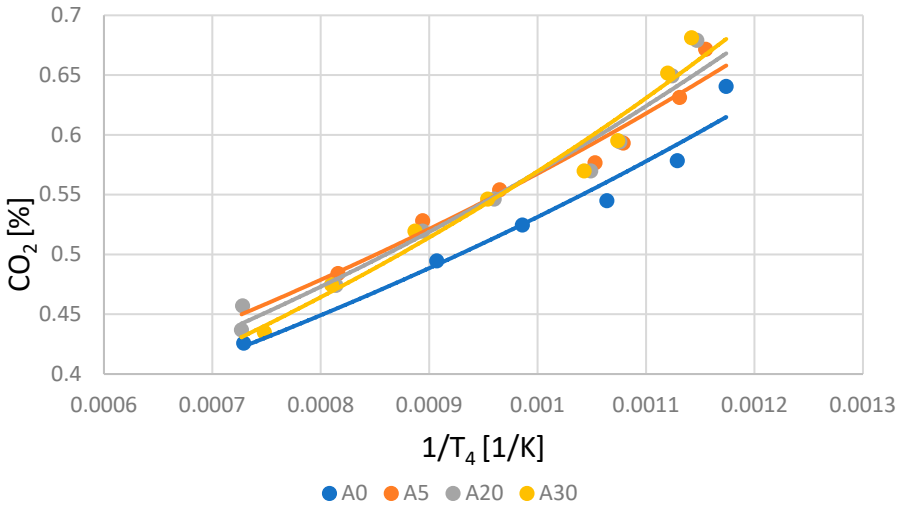

Figure 6. CO_2 concentration vs. inverted temperature.

Table 7. Empirically obtained values of the parameters of function (25) for the tested blends.

Fuel	R^2	$A_{CO2}m_f^pO_2^qt$	$E_{aCO2meas}/R$	$E_{aCO2meas}$
A0	0.9589	0.2293	−840	−6972
A5	0.9505	0.2425	−850	−7055
A20	0.9641	0.2259	−924	−7669
A30	0.9635	0.205	−1022	−8483

Figure 7 confirms that the A concentration in the tested fuels has a notable impact on EaCO2ch/EaCO2meas. Since a linear relationship between $E_{aCO2ch}/E_{aCO2meas}$ and the SAF concentration was confirmed, $E_{aCO2ch}/E_{aCO2meas}$ can be expressed by the following transformation of Equation (21):

$$-RT[\ln(AF)]/E_{ameas} + 1 = E_{aCO2ch}/E_{aCO2meas} \quad (36)$$

and

$$-RT[\ln(AF)]/E_{aCO2meas} + 1 = -0.0213c_{SAF} + 4.2659 \quad (37)$$

where c_{SAF} is the concentration of SAF in the tested fuels.

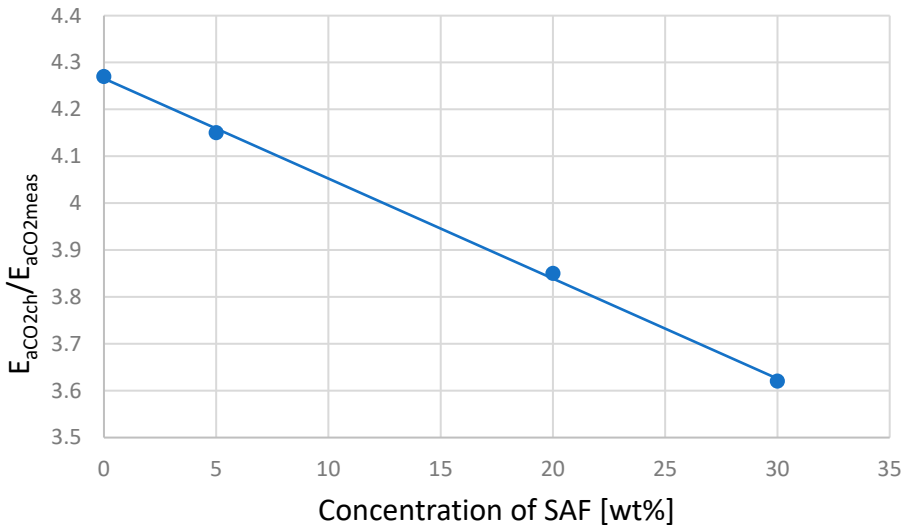

Figure 7. The relationship between $E_{aCO2ch}/E_{aCO2meas}$ and SAF concentration in the tested fuels.

4.3. E_{aCO} and α_{iCOch} Determined from Emission Measurements

The relationship between $[CO]_{meas}$ and m_f is shown in Figure 8 and Table 8. The curve for the A0 fuel is clearly different than those for the blends, including SAF.

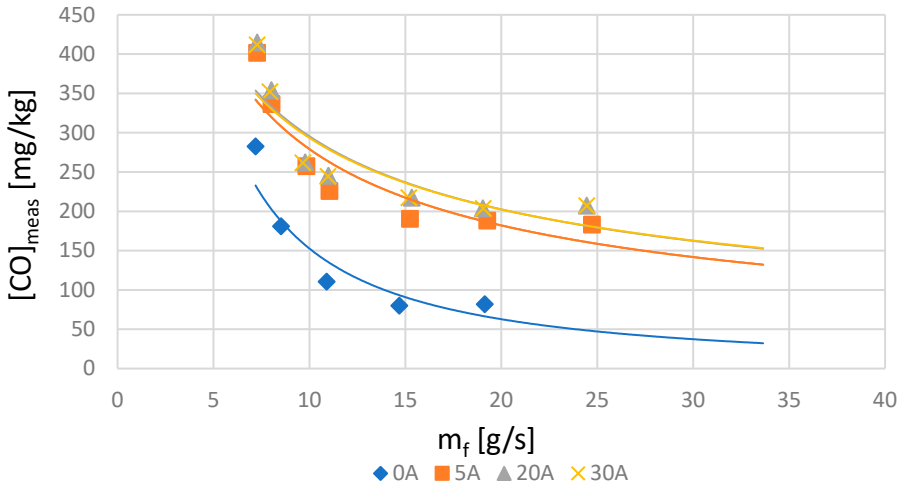

Figure 8. Relationship between $[CO]_{meas}$ and m_f for various concentrations of SAF.

Table 8. The parameters of functions $[CO]_{meas} = a_{CO}\ m_f^{n}$.

Fuel	R^2	a_{COmeas}	n
A0	0.9070	2918	−1.281
A5	0.8464	1153	−0.616
A20	0.8123	1036	−0.545
A30	0.8064	1007	−0.535

The relationship between CO and $1/T_4$ was used for the determination of the $(-E_{aCO} + E_{aCO2})_{ch}/R$ values for the tested fuels.

As shown in Figure 9, the concentration of CO in exhaust gases decreases when the temperature increases in the combustion chamber. This tendency should result from the dilution of exhaust gases by the air flowing through the engine (like in the case of the CO_2 concentration in exhaust gases).

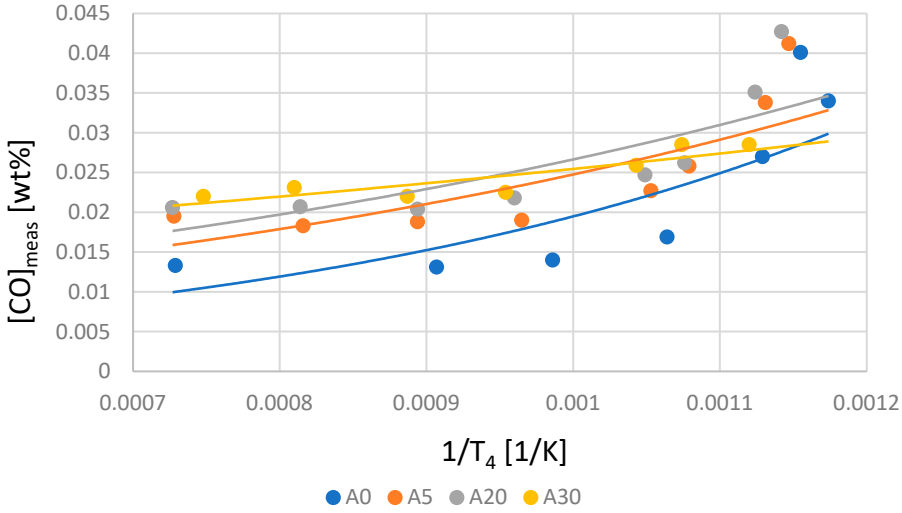

Figure 9. CO concentration vs. inverted combustion temperature.

The relatively low values of R^2 for relationships CO vs. $1/T_4$ in Table 9 indicate that the term $[\ln\{c_2[1 + e^t]/e^t\, c_5\} + \ln m_f^{np} - \ln(AF)]$ in Equation (32) is not constant for various m_f. Based on the E_{aCO2ch} values shown in Table 6, the values of E_{aCOch}/R were calculated.

Table 9. Empirically obtained parameters of the function from Equation (32).

Fuel	R^2	$(-E_{aCOch} + E_{aCO2ch})/R$	$\{c_2[1 + e^t]/e^t c_5\} m_f^n/(AF)$
A0	0.7411	2459	0.0017
A5	0.8464	1625	0.0049
A20	0.8123	1507	0.0059
A30	0.8064	734	0.0122

The E_{aCOch}/RT_{41} and am_f values were used for the $\alpha_{iCO}A_{CO}D_{CO}$ calculation. The results are shown in Figure 10 and Table 10.

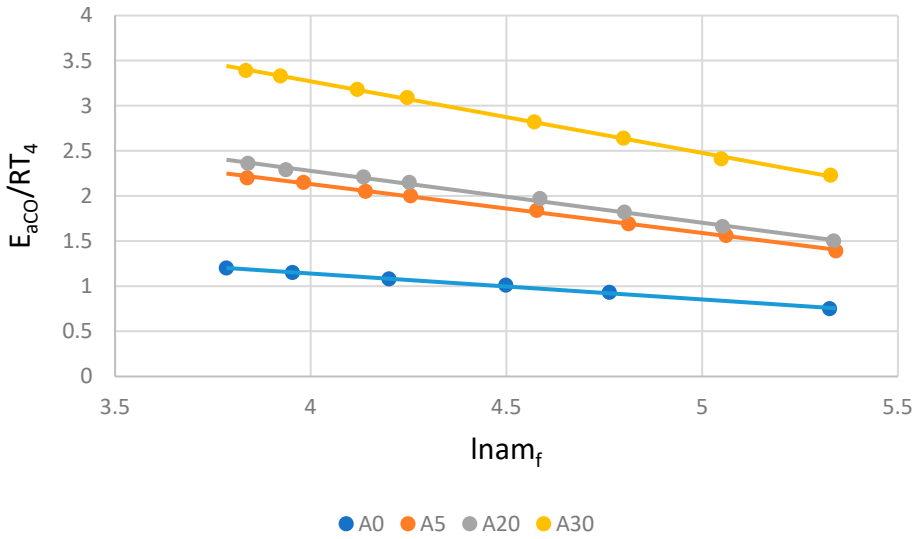

Figure 10. The relationship between E_{aCO}/RT_4 and $\ln am_f$.

Table 10. Empirically determined values of parameters that characterize the fuel's tendency to generate CO in exhaust gases (Equation (33)).

Fuel	R^2	$(E_{aCOch} - E_{aCO2ch})/R$	E_{aCOch}/R	E_{aCOch} [kJ/mol]	$\ln\alpha_{iCO}A_{CO}D_{CO}$	n_1
A0	0.9973	2459	1021	8.5	2.29	0.29
A5	0.9980	1625	1900	15.8	4.30	0.54
A20	0.9968	1507	2049	17.0	4.58	0.57
A30	0.9989	734	2971	24.7	6.44	0.79

5. Discussion

The results presented above indicate that the synthetic component introduced into the fossil-fuel Jet A-1 does not noticeably affect the operation of the DGEN 380 engine, since the relationship between thrust and fuel flow for all the tested fuels is practically the same. But, it has a significant impact on the combustion chemistry and emissions, i.e., CO_2 and CO. Two criteria were used to assess the impact of SAF content on the combustion chemistry and engine operating parameters:

- activation energy E_a related to the whole chain of combustion reactions;
- coefficient of reactivity α_i related to thrust F, fuel flow m_f, and constant rate determined for all chain of combustion reactions k.

Table 11 shows both criteria determined for fuels consisting of fossil Jet A-1 fuel (A0) and blends of this fuel and A synthetic component in concentrations of 5, 20, and 30 wt%.

Table 11. Parameters characterizing the impact of SAF content on the kinetic of combustion and their reactivity related to this process.

Fuel	E_{aCO2ch}/R	$\ln\alpha i_{CO2ch}A_{CO2}D_{CO2}$	$E_{aCO2meas}/R$	E_{aCOch}/R	$\ln\alpha i_{CO}A_{CO}D_{CO}$
A0	3590	7.90	−840	1021	2.29
A5	3528	7.94	−850	1900	4.30
A20	3554	7.96	−924	2049	4.58
A30	3707	8.09	−1022	2971	6.44

The activation energy determined for the entire combustion reaction chain cannot be interpreted in the same way as for individual chemical reactions. However, when comparing the E_{aCO2ch} and E_{aCOch} (Table 11) values obtained for the fuels with different chemical compositions, this value can be treated as a criterion for the similarity of reaction chains. Using this method of assessing the similarity of combustion reaction chains of fuels with different SAF content, it was found that (Figure 11):

- SAF in a concentration between 5 and 20 wt% has a negligible impact on the kinetics of the entire fuel combustion chain, since the E_{aCO2ch} values for all tested fuels are similar;
- SAF affects the kinetics of the reaction chain ending with the formation of CO.

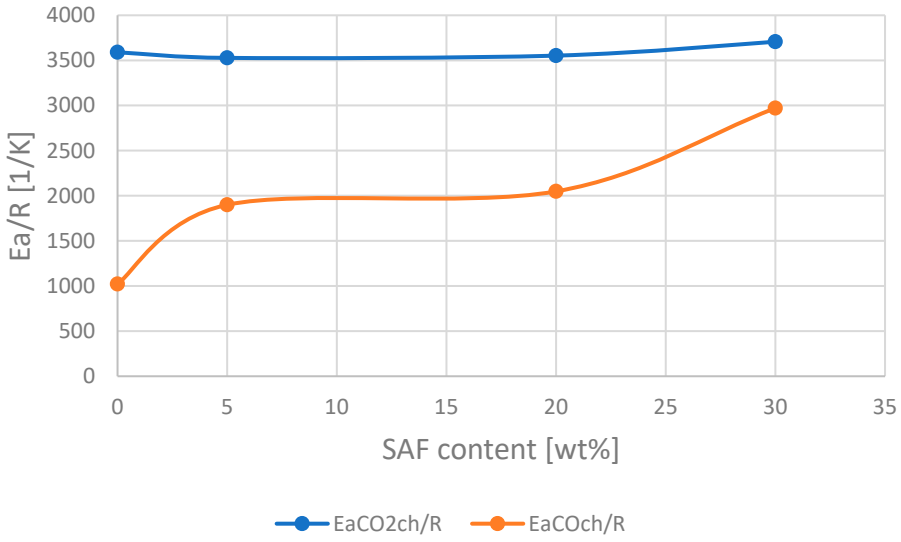

Figure 11. The relationship between E_a/R and SAF content in the tested fuel.

Considering that CO_2 formation is a subsequent reaction with CO as an intermediate product, the rate of the entire reaction chain is determined by the rate of the slowest reaction. Figure 11 indicates that, depending on SAF content, the activation energy of CO is from 70 to 20% smaller than that of CO_2. This suggests that:

- for CO_2 formation, the slowest stage is CO oxidation,
- for CO formation, the slowest is one of the reactions in the chain of fuel hydrocarbon oxidation to CO.

The above indicates that, regardless of the method for determining the value of E_a/R, the resultant activation energy of the combustion reaction to CO_2 increases with the increase in the concentration of component SAF. Conversely, the increase in the content of component SAF causes a decrease in the resultant activation energy of CO formation.

A comparison of the dependence of the calculated reactivity coefficient functions ($\ln\alpha_{iCO2}A_{CO2}D_{CO2}$) on the SAF content in the fuel leads to similar conclusions (Figure 12). Observing fuel combustion as one chain of reactions leading to the formation of CO_2 (this combustion product dominates quantitatively in the composition of exhaust gases), it can be concluded that the introduction of SAF in an amount of up to 30 wt% does not affect the reactivity coefficient. This seems obvious given the fact that the SAF component has been approved for use under the ASTM D4054 procedure. However, for CO emissions, an impact of the SAF content on the value of the reactivity coefficient function ($\ln\alpha_{iCO}A_{CO}D_{CO}$) is noticeable.

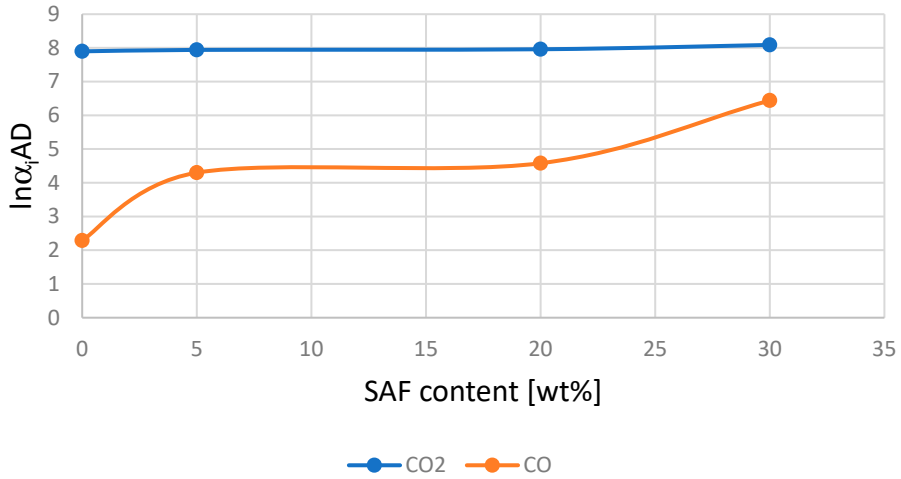

Figure 12. The impact of SAF content in tested fuels on the values of coefficient of reactivity α_i related to CO_2 and CO formation.

The results presented in Table 10 directly indicate a significant impact of SAF on CO emissions, E_{aCOch}/R changes from 1021 K to 2971 K and $\ln\alpha i_{CO}A_{CO}D_{CO}$ changes from 2.29 to 6.44, and indicate differences compared to Jet A-1 fuel in the kinetics of the reactions making up the fuel combustion chain in the DGEN 380 engine.

The regression results shown in Table 10 were used to formulate relationships between E_{aCO2Ch}/R, E_{aCOCh}/R, $\ln\alpha_{iCO2ch}A_{CO2}D_{CO2,}$ and $\ln\alpha_{iCO}A_{CO}D_{CO}$ and the SAF A concentration. On the basis of the results obtained for the A0, A20, and A30 fuels, the following relationships were formulated:

$$E_{aCO2Ch}/R = 0.57(\text{SAF concentration})^2 - 13.2(\text{SAF concentration}) + 3590 \quad (38)$$

$$E_{aCOCh}/R = 63.06(\text{SAF concentration}) + 962.7 \quad (39)$$

$$\ln\alpha_{iCO2ch}A_{CO2}D_{CO2} = 0.0003(\text{SAF concentration})^2 - 0.0021(\text{SAF concentration}) + 7.92 \quad (40)$$

$$\ln\alpha_{iCO}A_{CO}D_{CO} = 0.1349(\text{SAF concentration}) + 2.19 \quad (41)$$

It should be emphasized that the formulated equations refer to fuels containing the SAF A component and combustion in the DGEN 380 turbofan. With these relationships, the values of E_{aCO2Ch}/R, E_{aCOCh}/R, $\ln\alpha_{iCO2ch}A_{CO2}D_{CO2,}$ and $\ln\alpha i_{CO}A_{CO}D_{CO}$ were calculated for A5 fuel. The results are shown in Table 12. The models based on Equations (38) and (40) provided good agreement between the predicted and measured data. Meanwhile, those based on Equations (39) and (41) performed worse, since CO formation is not well modeled.

Table 12. The model validation results.

Parameter	Predicted	Empirically Determined
E_{aCO2Ch}/R	3538	3525
E_{aCOCh}/R	1278	1900
$\ln\alpha_{iCO2ch}A_{CO2}D_{CO2}$	7.92	7.94
$\ln\alpha_{iCO}A_{CO}D_{CO}$	2.86	4.30

6. Conclusions

The paper attempts to model the impact of the concentration of synthetic fuel on combustion in a turbofan engine. For this purpose, the α_i reactivity model, developed and verified in earlier tribochemical studies, was used. The proposed approach uses linear regression to determine the reactivity coefficients α_{iCO2} and α_{iCO}, describing the mechanism and kinetics of complete (to CO_2) and incomplete (to CO) combustion reactions. Due to the use of this model, quantities such as thrust and fuel flow were quantitatively related to the kinetics of the formation of exhaust gases.

To assess the impact of the synthetic component on combustion in the DGEN 380 engine, two criteria were used, namely the resultant activation energy determined for the entire chain of reactions ending with the production of CO_2 and CO function of the reactivity coefficient α_{iCO2} and α_{iCO}. It was found that SAF in the concentration range of up to 30 wt% does not affect fuel combustion to CO_2, while its impact is significant in relation to the combustion reaction to CO. The reactivity model led to calculating the coefficient of reactivity α_i expressed as $\ln\alpha_{iCO}A_{CO}D_{CO,}$ whose value changes between 2.29 for A0 and 6.44 for A30, while $\ln\alpha_{iCO2}A_{CO2}D_{CO2}$ changes between 7.90 for A0 and 8.08 for A30. The above results indicate the impact of the tested biofuel A on combustion chemistry and propose the following criteria for biofuel evaluation: E_{aCO2}, E_{aCO}, $\ln(\alpha_{iCO2ch}A_{CO2}D_{CO2})$, and $\ln\alpha_{iCO}A_{CO}D_{CO}$. The critical values of these criteria will be determined via further testing.

The presented assessment of fuel combustion is of a comparative nature, i.e., the calculated values of the reactivity coefficients for the blends containing the SAF component are compared to the values obtained for the fossil Jet A-1 fuel. Future work will be focused on linking the reactivity coefficients with a greater number of operational parameters, including those affecting engine durability and reliability.

Author Contributions: Conceptualization, A.K.; Methodology, A.K. and R.P.; Validation, J.M.; Formal analysis, A.K.; Investigation, R.P., B.G., R.J. and I.P.; Data curation, R.P.; Writing—original draft, A.K. and R.P.; Writing—review and editing, R.P. and T.B.; Visualization, R.P.; Supervision, T.B. All authors have read and agreed to the published version of the manuscript.

Funding: This research received no external funding.

Data Availability Statement: The original contributions presented in the study are included in the article, further inquiries can be directed to the corresponding authors.

Acknowledgments: We would like to thank Wojciech Dzięgielewski for his comments on an earlier version of the manuscript. Our special thanks are extended to the Military University of Technology in Warsaw (WAT) for providing the DGEN 380 turbofan.

Conflicts of Interest: The authors declare no conflict of interest.

Abbreviations

The following symbols and abbreviations are used in this manuscript:

a	slope in linear regression
CO	carbon monoxide
CO_2	carbon dioxide
F	thrust
ITWL	Air Force Institute of Technology in Warsaw

m_f	fuel flow
NH	High-pressure turbine speed
NL	Low-pressure turbine speed
O_2	oxygen
OEM	original equipment manufacturer
PLA	power lever angle
rpm	revolutions per minute
SAF	sustainable aviation fuel
SFC	specific fuel consumption
WESTT	Whole Engine Simulator Turbine Technology

References

1. Dahal, K.; Brynolf, S.; Xisto, C.; Hansson, J.; Grahn, M.; Grönstedt, T.; Lehtveer, M. Techno-economic review of alternative fuels and propulsion systems for the aviation sector. *Renew. Sustain. Energy Rev.* **2021**, *151*, 111564. [CrossRef]
2. Directive (EU) 2018/2001 of the European Parliament and of the Council of 11 December 2018 on the promotion of the use of energy from renewable sources. *Off. J. Eur. Union* **2018**, *328*, 82–209.
3. Yang, J.; Xin, Z.; Corscadden, K.; Niu, H. An overview on performance characteristics of bio-jet fuels. *Fuel* **2019**, *237*, 916–936. [CrossRef]
4. Kumal, R.R.; Liu, J.; Gharpure, A.; Vander Wal, R.L.; Kinsey, J.S.; Giannelli, B.; Stevens, J.; Leggett, C.; Howard, R.; Forde, M.; et al. Impact of biofuel blends on black carbon emissions from a gas turbine engine. *Energy Fuels* **2020**, *34*, 4958–4966. [CrossRef] [PubMed]
5. *ASTM D7566*; Standard Specification for Aviation Turbine Fuel Containing Synthesized Hydrocarbons. ASTM International: West Conshohocken, PA, USA, 2022.
6. *ASTM D4054*; Standard Practice for Evaluation of New Aviation Turbine Fuels and Fuel Additives. ASTM International: West Conshohocken, PA, USA, 2022.
7. Heyne, J.; Rauch, B.; Le Clercq, P.; Colket, M. Sustainable aviation fuel prescreening tools and procedures. *Fuel* **2021**, *290*, 120004. [CrossRef]
8. Zhang, C.; Hui, X.; Lin, Y.; Sung, C.-J. Recent development in studies of alternative jet fuel combustion: Progress, challenges, and opportunities. *Renew. Sustain. Energy Rev.* **2016**, *54*, 120–138. [CrossRef]
9. Kramer, S.; Andac, G.; Heyne, J.; Ellsworth, J.; Herzig, P.; Lewis, K.C. Perspectives on fully synthesized sustainable aviation fuels: Direction and opportunities. *Front. Energy Res.* **2022**, *9*, 782823. [CrossRef]
10. Reddy, V.J.; Hariram, N.P.; Maity, R.; Ghazali, M.F.; Kumarasamy, S. Sustainable e-fuels: Green hydrogen, methanol and ammonia for carbon-neutral transportation. *World Electr. Veh. J.* **2023**, *14*, 349. [CrossRef]
11. Peacock, J.; Cooper, R.; Waller, N.; Richardson, G. Decarbonising aviation at scale through synthesis of sustainable e-fuel: A techno-economic assessment. *Int. J. Hydrogen Energy* **2024**, *50*, 869–890. [CrossRef]
12. d'Amore, F.; Nava, A.; Colbertaldo, P.; Visconti, C.G.; Romano, M. Turning CO_2 from fuel combustion into e-fuel? Consider alternative pathways. *Energy Convers. Manag.* **2023**, *289*, 117170. [CrossRef]
13. Åkerblom, A.; Pignatelli, F.; Fureby, C. Numerical simulations of spray combustion in jet engines. *Aerospace* **2022**, *9*, 38. [CrossRef]
14. Kick, T.; Herbst, J.; Kathrotia, T.; Marquetand, M.; Braun-Unkhoff, M.; Naumann, C.; Riedel, U. An experimental and modeling study of burning velocities of possible future synthetic jet fuels. *Energy* **2012**, *43*, 111–123. [CrossRef]
15. Wang, K.; Xu, R.; Parise, T.; Shao, J.; Movaghar, A.; Lee, D.J.; Park, J.-W.; Gao, Y.; Lu, T.; Egolfopoulos, F.N.; et al. A physics-based approach to modeling real-fuel combustion chemistry—IV. HyChem modeling of combustion kinetics of a bio-derived jet fuel and its blends with a conventional Jet A. *Combust. Flame* **2018**, *198*, 477–489. [CrossRef]
16. Suchocki, T.; Lampart, P.; Klonowicz, P. Numerical investigation of a GTM-140 turbojet engine. *Open Eng.* **2015**, *5*, 1. [CrossRef]
17. Fulara, S.; Chmielewski, M.; Gieras, M. Variable geometry in miniature gas turbine for improved performance and reduced environmental impact. *Energies* **2020**, *13*, 5230. [CrossRef]
18. Gawron, G.; Białecki, T. Impact of a Jet A-1/HEFA blend on the performance and emission characteristics of a miniature turbojet engine. *Int. J. Environ. Sci. Technol.* **2018**, *15*, 1501–1508. [CrossRef]
19. Przysowa, R.; Gawron, B.; Białecki, T.; Łęgowik, A.; Merkisz, J.; Jasiński, R. Performance and emissions of a microturbine and turbofan powered by alternative fuels. *Aerospace* **2021**, *8*, 25. [CrossRef]
20. Curran, H.J. Developing detailed chemical kinetic mechanisms for fuel combustion. *P. Combust. Inst.* **2019**, *37*, 57–81. [CrossRef]
21. Meeks, E.; Ando, H.; Chou, C.P.; Dean, A.M.; Hodgson, D.; Koshi, M.; Lengyel, I.; Maas, U.; Naik, C.V.; Puduppakkam, K.V.; et al. New modeling approaches using detailed kinetics for advanced engines. In Proceedings of the 7th International Conference on Modeling and Diagnostics for Advanced Engine Systems, (COMODIA 2008), Sapporo, Japan, 28–31 July 2008. [CrossRef]
22. Kroyan, Y.; Wojcieszyk, M.; Kaario, O.; Larmi, M. Modeling the impact of sustainable aviation fuel properties on end-use performance and emissions in aircraft jet engines. *Energy* **2022**, *255*, 124470. [CrossRef]
23. Kaźmierczak, U.; Dzięgielewski, W.; Kulczycki, A. Miscibility of aviation turbine engine fuels containing various synthetic components. *Energies* **2022**, *15*, 6187. [CrossRef]

24. Yan, S.; Tang, G.; Zhou, C.Q.; Guo, X. Computational fluid dynamics modeling of combustion characteristics of a CH_4/O_2 combustor in a copper anode furnace. *ACS Omega* **2019**, *4*, 12449–12458. [CrossRef] [PubMed]
25. Nassini, P.C.; Pampaloni, D.; Meloni, R.; Andreini, A. Lean blow-out prediction in an industrial gas turbine combustor through a LES-based CFD analysis. *Combust. Flame* **2021**, *229*, 111391. [CrossRef]
26. Mansel, A.C.; Kahle, D.J.; Bellert, D.J. Calculating RRKM rate constants from vibrational frequencies and their dynamic interpretation. *Math. J.* **2017**, *19*, 1–20. [CrossRef]
27. Zhao, H.; Liu, H. *Breakup Morphology and Mechanisms of Liquid Atomization; Environmental Impact of Aviation and Sustainable Solutions*; IntechOpen: Rijeka, Croatia, 2019. [CrossRef]
28. *ARP 1533C*; Procedure for the Analysis and Evaluation of Gaseous Emission from Aircraft Engines. SAE International: Warrendale, PA, USA, 2016.
29. Cuoci, A.; Frassoldati, A.; Faravelli, T.; Ranzi, E. A computational tool for the detailed kinetic modeling of laminar flames: Application to C_2H_4/CH_4 coflow flames. *Combust. Flame* **2013**, *160*, 870–886. [CrossRef]
30. Wang, H.; Liu, B.; Xie, C.; Li, Y.; Cui, J.; Xing, L.; Wang, Z. Thermal decomposition of isopentanol: A theoretical calculation and kinetic modeling analysis. *Combust. Flame* **2022**, *245*, 112320. [CrossRef]
31. Kozakiewicz, A.; Kołodziejska, A.; Kieszek, R. Application of laboratory tests in numerical analysis for exhaust emissions in business jet engines. *Adv. Sci. Technol. Res. J.* **2023**, *17*, 21–35. [CrossRef]
32. *DGEN 380 BR Training. DSF-000008-A01 (Unpublished)*; Price Induction: Anglet, France, 2017.